

# Organic Secondary Ion Mass Spectrometry: Sensitivity Enhancement by Gold Deposition

A. Delcorte,\* N. Médard, and P. Bertrand

PCPM, Université catholique de Louvain, 1 Croix du Sud, B1348, Louvain-la-Neuve, Belgium

**Hydrocarbon oligomers, high-molecular-weight polymers, and polymer additives have been covered with 2–60 nmol of gold/cm<sup>2</sup> in order to enhance the ionization efficiency for static secondary ion mass spectrometry (s-SIMS) measurements. Au-cationized molecules (up to ~3000 Da) and fragments (up to the trimer) are observed in the positive mass spectra of metallized polystyrene (PS) oligomer films. Beyond 3000 Da, the entanglement of polymer chains prevents the ejection of intact molecules from a “thick” organic film. This mass limit can be overcome by embedding the polymer chains in a low-molecular-weight matrix. The diffusion of organic molecules over the metal surfaces is also demonstrated for short PS oligomers. In the case of high-molecular-weight polymers (polyethylene, polypropylene, PS) and polymer additives (Irganox 1010, Irgafos 168), the metallization procedure induces a dramatic increase of the fingerprint fragment ion yields as well as the formation of new Au-cationized species that can be used for chemical diagnostics. In comparison with the deposition of submonolayers of organic molecules on metallic surfaces, metal evaporation onto organic samples provides a comparable sensitivity enhancement. The distinct advantage of the metal evaporation procedure is that it can be used for any kind of organic sample, irrespective of thickness, opening new perspectives for “real world” sample analysis and chemical imaging by s-SIMS.**

Improving the qualitative and quantitative value of the information provided by the mass spectrum constitutes a major goal in the development of organic secondary ion mass spectrometry (SIMS).<sup>1</sup> In addition to the elaboration of more efficient spectral interpretation procedures, this objective can be pursued by investigating either different primary beam bombardment conditions or sample preparation methods. The present article is part of a study aimed at developing organic sample preparation routes that lead to an improvement of the performance of SIMS via, for instance, the enhancement of the useful signal, the access to a broader mass range, or the reduction of molecule fragmentation. To proceed to a systematic investigation in this domain, it is crucial to establish a basic understanding of the emission processes in

these new systems. Therefore, throughout the article, we also place the emphasis on the fundamental aspects of organic solid sputtering.

The specific route investigated hereafter consists of the evaporation of a small quantity of metal on the sample surface.<sup>2</sup> In principle, the presence of metal at the sample surface should play a role primarily in the ionization step of the emission process, for instance, by changing the work function of the surface and providing an external source of ionizing particles. In the context of the SIMS analysis, it is useful to compare surface metallization with the sister method that consists of casting organic molecules on metal substrates. In the latter case, the molecular or fragment species ejected from the surface recombine with metal particles so that the metal substrate constitutes an external “reservoir” of ionizing agent. The heavy metal substrate also facilitates molecular desorption via a very efficient upward reflection of the projectile momentum. This method has been abundantly used and commented on in the literature over the last two decades.<sup>3–14</sup> Its major advantage is that it allows analysts to expand the mass range of SIMS for (sub)monolayers of organic materials, up to ~10 000 Da for the parentlike ions of limited-size molecules<sup>6</sup> and a few thousand Daltons for fragments of larger polymers.<sup>7</sup> A significant drawback is that only (sub)monolayer films, carefully prepared from very dilute solutions, can be analyzed using this sample preparation procedure. In other words, the method is useless for samples that cannot be prepared as ultrathin films, such as compounds with a very poor solubility, and for real world surfaces that must be analyzed as such. In those cases, the evaporation of metal atoms on the sample surface, if it proves successful for the analysis, certainly constitutes an interesting alternative.

- (2) Travaly, Y.; Bertrand, P. *Surf. Interface Anal.* **1995**, *23*, 328.
- (3) Grade, H.; Winograd, N.; Cooks, R. G. *J. Am. Chem. Soc.* **1977**, *99*, 7725.
- (4) Grade, H.; Cooks, R. G. *J. Am. Chem. Soc.* **1978**, *100*, 5615.
- (5) Bletsos, I. V.; Hercules, D. M.; van Leyen, D.; Benninghoven, A. *Macromolecules* **1987**, *20*, 407.
- (6) Bletsos, I. V.; Hercules, D. M.; van Leyen, D.; Hagenhoff, B.; Niehuis, E.; Benninghoven, A. *Anal. Chem.* **1991**, *63*, 1953.
- (7) Zimmerman, P. A.; Hercules, D. M.; Benninghoven, A. *Anal. Chem.* **1993**, *65*, 983.
- (8) Benninghoven, A.; Hagenhoff, B.; Niehuis, E. *Anal. Chem.* **1993**, *65*, 630A.
- (9) Benninghoven, A. *Surf. Sci.* **1994**, *299/300*, 246.
- (10) Xu, K.; Proctor, A.; Hercules, D. M. *Mikrochim. Acta* **1996**, *122*, 1.
- (11) Nicola, A. J.; Muddiman, D. C.; Hercules, D. M. *J. Am. Soc. Mass Spectrom.* **1996**, *7*, 467.
- (12) Pleul, D.; Simon, F.; Jacobasch, H.-J. *Fresenius' J. Anal. Chem.* **1997**, *357*, 684.
- (13) Gusev, A. I.; Choi, B. K.; Hercules, D. M. *J. Mass Spectrom.* **1998**, *33*, 480.
- (14) Keller, B. A.; Hug, P. In *Secondary Ion Mass Spectrometry, SIMS XII Proceedings*; Benninghoven, A., Bertrand, P., Migeon, H.-N., Werner, H. W., Eds.; Elsevier: Amsterdam, 2000; pp 749, 885.

\* To whom correspondence should be addressed. Phone: 32-10-473582. Fax: 32-10-473452. E-mail: delcorte@pcpm.ucl.ac.be.

(1) *Secondary Ion Mass Spectrometry, SIMS XII Proceedings*; Benninghoven, A., Bertrand, P., Migeon, H.-N., Werner, H. W., Eds.; Elsevier: Amsterdam, 2000.

To our knowledge, the literature concerning surface metallization as a sample preparation route for SIMS analysis is relatively scarce,<sup>15–20</sup> and the potential of the method has not been fully explored yet. The first couple of reports describe the covering of polymer samples by a thick, patterned silver overlayer (100–500 nm), using a TEM grid as a mask during the metal evaporation step.<sup>15,16</sup> Even though the authors suggest that 150-nm-thick silver patterns provide the best results, from the viewpoint of SIMS analysis, it appears to us as if the large regions covered by the thick metal layers had been sacrificed. Our approach, via the evaporation of minute amounts of metal over the whole sample area, is rather in the line of the reports of refs 18 and 19. These reports certainly show that silver metallization of organic samples induces the cationization of sputtered oligomers and polymer fragments, demonstrating the interest of the method. Nonetheless, the study presented in refs 18 and 19, however detailed, does not provide an estimate of the amount of metal (Ag) deposited. In addition, the results concerning thin layers (including monolayers) of molecules are ambiguous, because the samples are deposited on a substrate of the same nature as the evaporated metal. Therefore, we believe that a new assessment of the method, including fundamental insights into ion formation mechanisms, is desirable.

In this report, gold metallization is performed for a set of organic surfaces, including oligomer samples belonging to the polystyrene family, bulk samples of high-molecular-weight polymers, and polymer additives. In the course of the study, molecular analytes dissolved in a matrix have also been investigated for fundamental purpose. The metal used here is gold, because it is known as a good cationizing agent,<sup>21</sup> it is more noble than silver (not easily oxidized), and it has a single isotope.

The results part of the article begins with an in-depth evaluation of the method for the analysis of synthetic oligomer molecules in the mass range 0–10 000 Da, the traditional application field of the sister cationization procedure using metal substrates. It is shown that fingerprint fragments as well as entire molecules can be cationized, with some restrictions for higher mass oligomers. Indeed, chain entanglement in pure oligomer layers becomes a problem when the molecular weight exceeds ~3000 Da. The optimum evaporated gold quantity, important for practical applications, is determined and commented. To gain a better understanding of the metallized sample surfaces, we investigate the issues of the gold layer structure/stability and the diffusion of organic molecules on top of gold surfaces. After this detailed fundamental

investigation, the discussion opens toward practical case studies involving bulk polymeric samples and polymer additive-containing films. In these sections, our major goal is to demonstrate the tractability and the interest of the gold evaporation sample preparation procedure for solving problems related to real world samples. In particular, the value of the method is demonstrated for the analysis of bulk, high-molecular-weight polyolefins (polyethylene, polypropylene, and polystyrene) as well as the investigation of antioxidant molecule segregation in polymer surfaces.

## MATERIALS AND METHODS

**Samples.** The nature and origin of the chosen samples as well as their preparation method are listed in Table 1. Samples of various organic molecules, including four low-molecular-weight polymers belonging to the polystyrene family and a polymer additive (Irganox 1010), were dissolved to a concentration of 1 mg/mL. Three high-molecular-weight bulk polymers, polyethylene (PE), polypropylene (PP), and polystyrene (PSHM), were used as such. A fourth high-molecular-weight polymer sample, poly(ethylene terephthalate/ethylene isophthalate) (PETI) was dissolved in chloroform with 1 wt % of Irgafos 168 antioxidant, spin-cast (20 000 rpm<sup>-1</sup>; 5000 rpm; 60 s) on a clean silicon wafer, and aged for 6 months in air. The other dissolved molecules were cast on ~0.25 cm<sup>2</sup> substrates by depositing a droplet of the solution on the supports and allowing the solvent to evaporate. As indicated in Table 1, the first series of samples was cast on clean silicon wafers; the second series was cast on gold-metallized supports. In a complementary series of experiments, we prepared toluene solutions containing 0.1 mg/mL of analyte and 1 mg/mL of matrix. We chose tetraphenyl-naphthalene (TPN) as a matrix, because it is very close to polystyrene from a chemical viewpoint and provides a clear molecular signal in SIMS. These solutions were also cast on clean silicon and gold-metallized supports. The metallized substrates were prepared by first evaporating a 5-nm titanium adhesive layer and then a 100 nm gold layer onto clean silicon wafers. Conversely, the organic samples cast on clean silicon wafers as well as the bulk polymers were metallized afterward by evaporating gold at a rate of 2, 6, 20, or 60 nmol/cm<sup>2</sup> (the equivalent of a 2-, 6-, 20-, or 60-Å gold layer) onto their top surface. Prior to organic sample deposition/gold metallization, all of the silicon substrates were rinsed in 2-propanol and hexane (p.a. grade; Vel).

The evaporation was carried out in an Edwards evaporator at an operating pressure of ~10<sup>-6</sup> mbar and a deposition rate of 0.1 nm/s. The deposited metal amount was measured using a quartz crystal monitor, and the given values corresponded to the assumption that the sticking coefficient is the same on the monitor and the organic samples. Because of this hypothesis, the deposited amount might be overestimated,<sup>22</sup> and the quoted metal quantities provided along the article must be considered as indicative rather than accurate values. Despite this uncertainty, the deposition conditions were reproducible, which validates the method.

**Secondary Ion Mass Spectrometry (SIMS).** The secondary ion mass analyses were performed in a PHI-EVANS time-of-flight SIMS (TRIFT 1) using a 15 keV Ga<sup>+</sup> beam (FEI 83-2 liquid metal ion source; ~600 pA DC current; 22-ns pulse width bunched down

- (15) Linton, R. W.; Mawn, M. P.; Belu, A. M.; DeSimone, J. M.; Hunt, M. O., Jr.; Menciloglu, Y. Z.; Cramer, H. G.; Benninghoven, A. *Surf. Interface Anal.* **1993**, *20*, 991.
- (16) Belu, A. M.; Mawn, M. P.; Linton, R. W. In *Secondary Ion Mass Spectrometry, SIMS IX Proceedings*; Benninghoven, A., Nihei, Y., Shimizu, R., Werner, H. W., Eds.; Wiley: New York, 1994; p 780.
- (17) Karen, A.; Benninghoven, A. In *Secondary Ion Mass Spectrometry, SIMS IX Proceedings*; Benninghoven, A., Nihei, Y., Shimizu, R., Werner, H. W., Eds.; Wiley: New York, 1994; p 788.
- (18) Simon, C. Ph.D. Thesis, University of Metz, 1996.
- (19) Simon, C.; Saldi, F.; Migeon, H.-N. In *Polymer-Solid Interfaces: From Model to Real Systems*; Pireaux, J.-J., Delhalle, J., Rudolf, P., Eds.; Presses Universitaires de Namur: Namur, 1998; p 411.
- (20) Yanashima, H.; Sado, M.; Minobe, M. In *Secondary Ion Mass Spectrometry, SIMS X Proceedings*; Benninghoven, A., Hagenhoff, B., Werner, H. W., Eds.; Wiley: New York, 1997; p 751.
- (21) Delcorte, A.; Wojciechowski, I.; Gonze, X.; Garrison, B. J.; Bertrand, P. *Int. J. Mass Spectrom.* **2002**, *214*, 213.

- (22) Novak, S.; Mauron, R.; Dietler, G.; Schlapbach, L. In *Metallized Plastics 2: Fundamental and Applied Aspects*; Mittal, K. L., Ed.; Plenum Press: New York, 1991; p 233.

Table 1. Description of the Samples<sup>a</sup>

molecule	acronym	$M_n$ (Da)	source	sample nature	[Si]/M/ Au	Au/M	$\frac{[\text{Si}]}{[\text{M} + \text{TPN}]}$ Au	Au/ [M + TPN]
Hydrocarbons								
tetraphenyl naphthalene	TPN	433	Sigma-Aldrich NV/SA Bornem	cast (toluene)		+	n/a	n/a
Additives								
Irgafos 168 [1-tris(2,4-di- <i>tert</i> -butylphenyl) phosphite]	I168	646	Ciba Specialty Chemicals Inc., Basel	PETI <sup>b</sup> /I168 blend in chloroform, spin-cast	+		n/a	n/a
Irganox 1010 [octadecyl-3-(3,5-di- <i>tert</i> -butyl-4-hydroxyphenyl) propionate]	I1010	1176	Ciba Specialty Chemicals Inc., Basel	cast (toluene)	+	+		
Low-MW Polymers								
polystyrene	PS700	700	Scientific Polymer Products Inc., Ontario	cast (toluene)	+	+		
polystyrene	PS2180	2180	Scientific Polymer Products Inc., Ontario	cast (toluene)	+	+	+	+
poly(4-methyl styrene)	P4MS	3930	University of Louvain	cast (toluene)	+	+	+	+
polystyrene	PS8000	8000	Scientific Polymer Products Inc., Ontario	cast (toluene)	+	+	+	+
High MW Polymers								
low-density polyethylene	PE	unknown	Vel	bottle	+	n/a	n/a	n/a
polypropylene	PP	unknown	Shell Research, Louvain-la-Neuve	film	+	n/a	n/a	n/a
polystyrene	PSHM	unknown	Vel	Petri dish	+	n/a	n/a	n/a

<sup>a</sup> The last four columns indicate which type of structures have been elaborated (+) with each sample (see Experimental Section). <sup>b</sup> Poly(ethylene terephthalate-ethylene isophthalate).

to  $\sim 1$  ns; 4 kHz repetition rate).<sup>23</sup> The experimental setup has been described in detail elsewhere.<sup>24</sup> To improve the measured intensities, the secondary ions were postaccelerated by a high voltage (7 kV) in front of the detector. All of the TOF-SIMS spectra in the mass range  $0 < m/z < 10\,000$  were obtained from 1200-s acquisitions on a  $260 \times 260 \mu\text{m}^2$  sample area, which corresponds to a fluence of  $2.6 \times 10^{11}$  ions/cm<sup>2</sup>, ensuring static bombardment conditions. In the discussion, all of the quoted secondary ion intensities correspond to peak areas, and they are expressed in counts.

## RESULTS AND DISCUSSION

The goal of this article is to assess the interest of organic sample metallization for SIMS analyses. The discussion is divided into three sections. The first section, extensively developed, investigates the case of a series of oligomers from the polystyrene family, with a mass in the range 0–10 000 Da. The second and third sections address the effect of gold evaporation on the mass spectra of high polymers and polymer additives (antioxidants). For oligomers and additives, SIMS is technically able to detect the parent ion, which constitutes the ultimate signature of the molecule, whereas in the case of high polymers, it can only provide access to the fragmentation products sputtered from the sample.

**Hydrocarbon Oligomers.** The new features induced in the mass spectrum as a result of the evaporation of gold on the sample

surface are illustrated using the PS sample family. As indicated in Table 1, the considered molecules are PS oligomers with molecular weights in the range 700–8000 Da and a poly(4-methylstyrene) sample of  $\sim 3900$  Da. The low-mass and high-mass ranges of the positive mass spectra are discussed separately.

**Fingerprint Region of the Mass Spectrum.** The low-mass range of the positive mass spectrum of metallized PS2180 is presented in the first two vignettes of Figure 1. This sample received a gold dose of 20 nmol/cm<sup>2</sup>. The silicon support appears homogeneously covered by the PS sample, because there is no silicon signal in the mass spectrum. According to previous studies of the information depth using polymer-covered silicon substrates,<sup>25</sup> this observation confirms that the thickness of the organic layer reaches at least 10 nm.

In the mass range 0–200 Da, the dominant peak is by far  $\text{C}_7\text{H}_7^+$ , resulting most probably from a recombination of the  $\text{C}_7\text{H}_6$  neutral fragments with a neighboring hydrogen atom or a proton.<sup>26</sup> The intensity of the  $\text{C}_7\text{H}_7^+$  ion is close to  $10^6$  counts, but it is only  $10^5$  counts for the same sample deposited on silicon and sputtered with the same primary ion fluence.<sup>27,28</sup> Other characteristic peaks of PS, built on either one or two styrene repeat units, are  $\text{C}_8\text{H}_9^+$  ( $m/z = 105$ ),  $\text{C}_9\text{H}_9^+$  ( $m/z = 115$ ), and  $\text{C}_{13}\text{H}_{13}^+$  ( $m/z = 193$ ). At

(25) Delcorte, A. In *ToF-SIMS: Surface Analysis by Mass Spectrometry*; Vickerman, J. C., Briggs, D., Eds.; SurfaceSpectra/IM Publications: Manchester, 2001; p 161.

(26) Delcorte, A.; Vanden Eynde, X.; Bertrand, P.; Vickerman, J. C.; Garrison, B. J. *J. Phys. Chem. B* **2000**, *104*, 2673.

(27) Vanden Eynde, X.; Jérôme, R.; Bertrand, P. *Macromolecules* **1997**, *30*, 6407.

(28) Vanden Eynde, X. Ph.D. Thesis, Université Catholique de Louvain, 1999.

(23) Schueler, B. W. *Microsc. Microanal. Microstruct.* **1992**, *3*, 119.

(24) Delcorte, A.; Vanden Eynde, X.; Bertrand, P.; Reich, D. F. *Int. J. Mass Spectrom.* **1999**, *189*, 133.

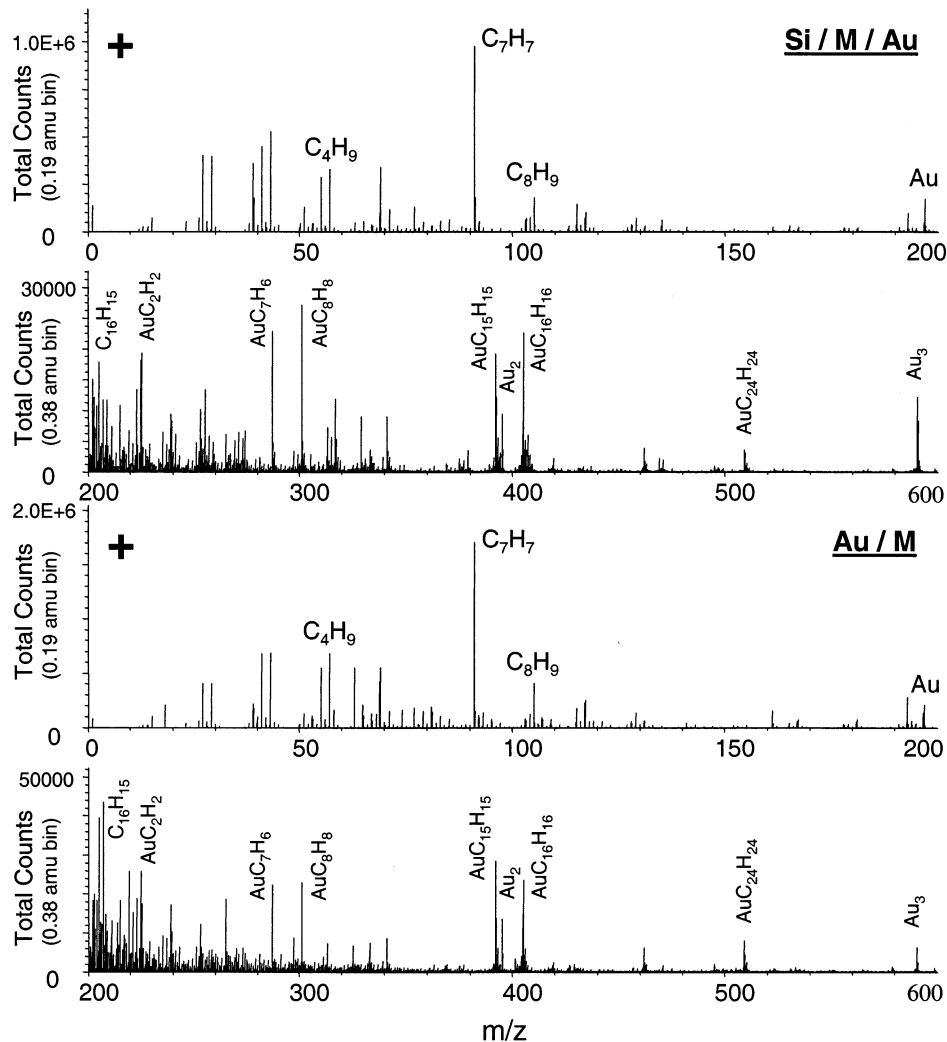


Figure 1. Low and intermediate mass range of the positive secondary ion mass spectrum of PS2180. Top spectrum, Au-metallized (20 nmol/cm<sup>2</sup>) sample; bottom spectrum, submonolayer on a gold substrate.

lower masses, the saturated hydrocarbon series might be related to the butyl chain end of the oligomers or to a contamination by small hydrocarbon molecules during the sample preparation procedure. These saturated peaks are present in the spectra of the same sample spin-coated on silicon wafers<sup>27,29</sup> but with a weaker intensity, suggesting that the sample preparation route used here introduces some additional contamination. As expected, the metallized sample exhibits a clear Au peak at  $m/z = 197$ .

In the mass range 200–600 Da, a new series of peaks emerges on the spectrum of the metallized PS (Figure 1, second frame) with respect to pristine PS. In addition to gold clusters ( $m/z = 394, 591$ ), homologues of the above-mentioned  $C_7H_7^+$  and  $C_8H_9^+$ , but with a gold atom instead of a hydrogen atom in the role of the cationizing agent, can be seen at  $m/z = 287$  ( $AuC_7H_6^+$ ) and  $m/z = 301$  ( $AuC_8H_8^+$ ). The latter peak is the Au cationized monomer of PS. Gold-cationized dimers ( $AuC_{16}H_{16}^+$ ) and trimers ( $AuC_{24}H_{24}^+$ ) are also present at very significant intensities. The peak at  $m/z = 392$ ,  $AuC_{15}H_{15}^+$ , is also characteristic of the PS structure. Its closer equivalent among the regular peaks of PS is  $C_{15}H_{13}^+$ .

For comparison, the third and fourth frames of Figure 1 show the low-mass range of the mass spectrum corresponding to a submonolayer of the same PS sample cast on a gold surface. Except for a few minor peaks, the spectrum is very similar in nature to that of the thicker PS layer covered with gold, shown in the first two frames. The same hydrocarbon and Au-cationized hydrocarbon fragments are observed, and the gold clusters are present in both cases. A noticeable difference concerns the intensities of sputtered ions, which are  $\sim 2$  times larger for the submonolayer cast on gold in the mass range 0–200 Da. The enhancement is not clear in the range 200–600 Da, especially for Au-cationized species. We can safely state that, for organometallic characteristic peaks in this mass range, the two preparation methods provide almost equivalent results.

In summary, with respect to pristine PS samples,<sup>29</sup> the metallization procedure enhances the fingerprint fragment intensities by at least 1 order of magnitude. The first two frames of Figure 1 also demonstrate that the low-mass spectrum of metallized PS sample exhibits a number of additional fragments that are also characteristic of polystyrene but require a recombination with an Au atom to become cations and be detected in SIMS. These new characteristic peaks are certainly valuable for the analyst and,

(29) *The Static SIMS Library*; Vickerman, J. C., Briggs, D., Henderson, A., Eds.; SurfaceSpectra: Manchester, 1997.

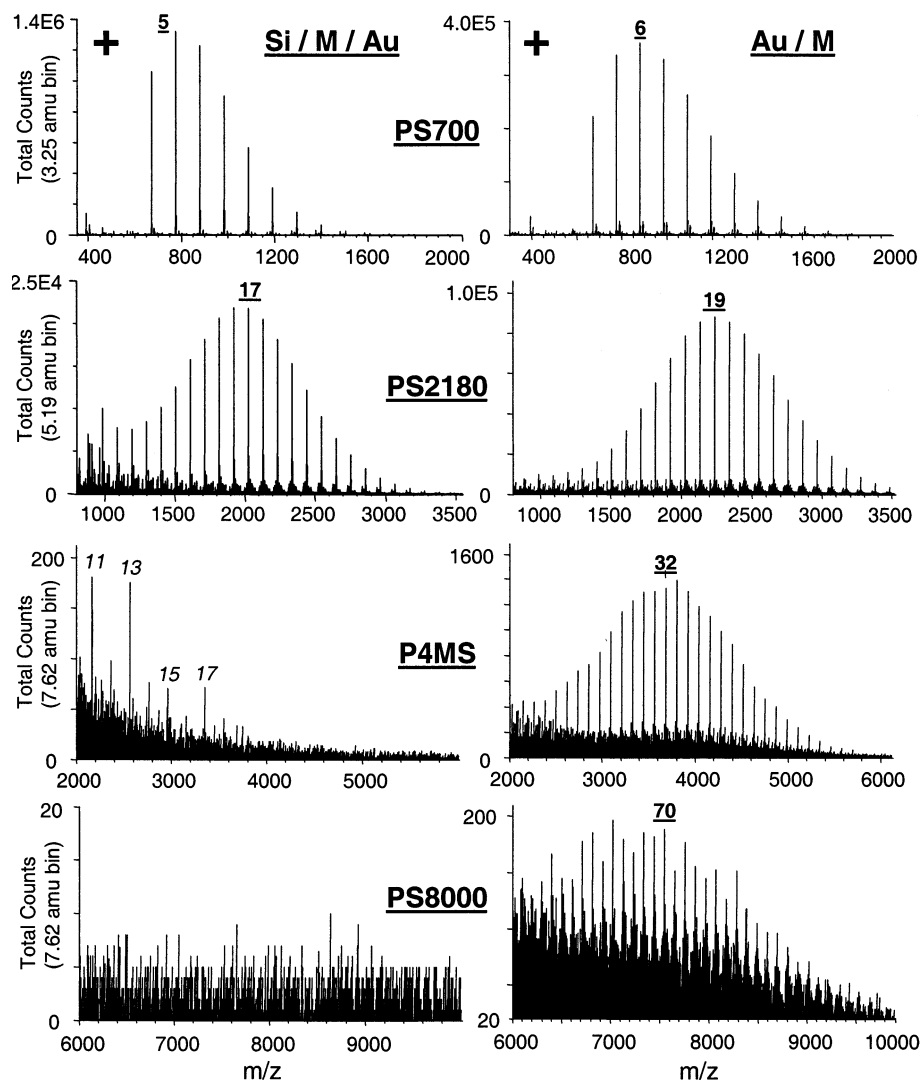


Figure 2. High-mass range of the positive secondary ion mass spectra of PS700, PS2180, P4MS, and PS8000. First column, Au-metallized ( $20 \text{ nmol/cm}^2$ ) samples; second column, submonolayers on gold substrates. The underlined numbers indicate the repeat unit number of the oligomer at the maximum of the distribution. The number of atoms in the Au clusters are in italic.

therefore, might alone justify the use of metallization as a sample preparation method.<sup>30</sup> Casting the sample on a gold surface, however, provides basically the same information. Therefore, the distinct strength of the metallization procedure resides more in the fact that it allows analysts to study thick layers as well as monolayers or submonolayers. It is, in this sense, less sample-dependent. The following subsection investigates the interest of the method for the direct investigation of entire molecules.

**Cationization Region of the Mass Spectrum.** In the first column of Figure 2, we present the parent ion region of the mass spectrum for four Au-covered samples belonging to the polystyrene family. These polymers are listed in Table 1, and their number average molecular weights are 700, 2180, 3930, and 8000. The first important observation is that the Au-cationized molecules are present in the spectrum only for the two lighter PS samples and not for the P4MS and PS8000 samples. In particular, only gold cluster peaks emerge from the noise in the parent ion mass range of the P4MS spectrum.

For comparison, the mass spectra of the same molecules deposited as submonolayers on bare gold surfaces are shown in the second column of Figure 2. In this case, the mass distribution of Au-cationized oligomers is apparent for all of the considered molecules. Another difference is the absolute intensity of the sputtered ions. The peaks of the mass distribution are, on average, 3–4 times more intense for the Au-covered layer in the case of PS700. For PS2180, the situation is reversed: the distribution is  $\sim 4$  times more intense with the submonolayer sample. In addition, the shapes of the PS700 and PS2180 mass distributions are affected by the sample preparation procedure. In the case of PS2180, the distribution peaks at 19 styrene repeat units and extends significantly beyond 3000 Da for the submonolayer on gold, but it peaks at 16–17 repeat units and vanishes beyond 3000 Da for the Au-covered film. The parent ion mass distribution observed for the Au-covered PS2180 sample is also asymmetric. It is probably polluted in the 1000–1500 Da mass range by large molecular fragments retaining the *sec*-butyl chain end (see discussion in ref 21).

(30) Ruch, D.; Boes, C.; Zimmer, R.; Muller, J. F.; Migeon, H.-N. *Appl. Surf. Sci.*, in press.

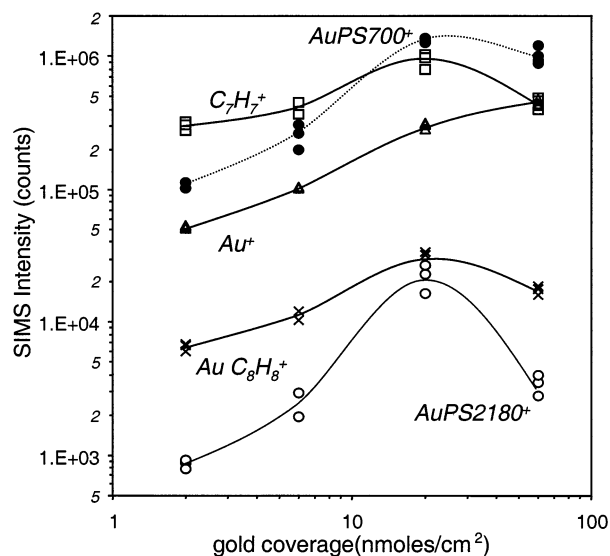


Figure 3. Evolution of the intensity of PS700 and PS2180 secondary ion peaks as a function of the deposited gold quantity (from 2 to 60 nmol/cm<sup>2</sup>). The Au<sup>+</sup>, C<sub>7</sub>H<sub>7</sub><sup>+</sup>, and AuC<sub>8</sub>H<sub>8</sub><sup>+</sup> curves correspond to fragments sputtered from PS2180.

All of these observations suggest either the action of diffusion processes at the surface, the effects of chain entanglement in the Au-covered molecular film, or simply the relative inefficiency of keV projectiles to desorb several kDa molecules from a thick organic sample, three phenomena that can be disregarded in submonolayer samples. The explanation of these observations is investigated in the next subsections. From the viewpoint of the SIMS analyst, the fact that molecules larger than 3 kDa cannot be detected from Au-covered films and the sample-preparation-dependence of the mass distribution shapes constitute limitations. In particular, the determination of the average molecular weight for synthetic oligomer samples should not be performed using metallized films of these molecules. Nevertheless, it is important to restate here that the metallization procedure still provides a drastic qualitative improvement for such oligomer films in comparison with the direct analysis of pristine (nonmetallized) samples, in which no molecular ions are detected at all. Besides, the observation that subkilodalton molecular ions are more efficiently sputtered from Au-covered films means the metallization procedure should be preferred for the analysis of molecules in this mass range.

**Influence of the Evaporated Gold Quantity.** To establish the best conditions for cationization, we monitored the variation of secondary ion absolute intensities as a function of the evaporated gold quantity from 2 to 60 nmol/cm<sup>2</sup>. The results are displayed in Figure 3 for various ions sputtered from PS2180 and for the cationized 5-mer sputtered from PS700. For comparison, Figure 3 also shows the evolution of the gold monocation peak. The gold monocation signal increases almost linearly with gold coverage up to 20 nmol/cm<sup>2</sup> (slope close to 1 in the log–log plot) and continues to increase with a softer slope afterward. The intensity of the tropyllium (C<sub>7</sub>H<sub>7</sub><sup>+</sup>) ion reaches a maximum around 20 nmol/cm<sup>2</sup> and decreases significantly for larger gold doses. Gold-cationized fragment (AuC<sub>8</sub>H<sub>8</sub><sup>+</sup>) and molecule (AuM<sup>+</sup>) intensities also increase monotonically over a wide range of coverage (from 2 to 20 nmol/cm<sup>2</sup>). In particular, the AuM<sup>+</sup> intensities increase

by more than 1 order of magnitude in this coverage range for both the 5-mer sputtered from PS700 (AuPS700) and the 18-mer desorbed from PS2180 (AuPS2180). Beyond the maximum, however, the evolution of these two peak intensities is different. Between 20 and 60 nmol/cm<sup>2</sup>, the intensity of the 18-mer decreases by almost 1 order of magnitude, whereas that of the 5-mer decreases by less than a factor of 2.

The fact that the gold-cationized complex intensities reach their maximum at 20 nmol/cm<sup>2</sup> justifies the use of this evaporated gold quantity in most of our experiments. The value of 20 nmol/cm<sup>2</sup> corresponds to an equivalent uniform metal layer thickness of ~20 Å (6–7 atomic layers assuming a sticking coefficient equal to 1). The observation of intensity maximums for this gold quantity is difficult to explain considering a uniform metal coverage, because such a thick layer should block the emission of buried organic fragments and molecules. On the other hand, the results can be satisfactorily interpreted assuming that the evaporated gold atoms form clusters or islands surrounded by bare organic surfaces. The fact that the 5-mer intensity (AuPS700) is sustained beyond the maximum, in contrast with the 18-mer intensity (AuPS2180), might be related to the pronounced diffusion of these small molecules on top of the gold layer, providing a large amount of material for cationization. In comparison, the much slower 18-mers might be buried under the gold surfaces and unable to cover them. The structure of the gold-covered surface and the issue of molecule diffusion are investigated in the following subsections.

**Structure and Stability of the Layer.** Information about the formation and evolution of the evaporated gold layer can be found in the secondary ion mass spectra in parallel with other inputs from the literature. Figure 4 shows a set of negative ion mass spectra corresponding to different states of a PS700 film covered with gold (6 nmol/cm<sup>2</sup>). The first frame (Figure 4a) is a spectrum measured 1 h after evaporation of the metal on the sample. In addition to a few intense peaks at low mass, the spectrum consists mainly of gold clusters containing up to at least 40 atoms. The same pattern of gold clusters is observed in the negative mass spectrum of all the analyzed molecules, including Irganox 1010, irrespective of the molecular weight or exact chemistry of the compound. It looks qualitatively similar to the cluster series displayed in the spectrum of Figure 4b, which arises from a sputter-cleaned gold surface. In the case of bare gold, however, the presence of clusters larger than 20 atoms is difficult to assess using the mass spectrum. In that sense, it appears easier to sputter large gold clusters from a Au-evaporated organic surface than from a pure gold surface, probably because the binding energy of the clusters to the surface is lower in the first case.

The direct implication of Figure 4a is that the freshly metallized PS700 surface is covered with gold clusters forming islands or a continuous gold layer. The complete coverage of the sample by a uniform gold film, which should be two or three monolayers thick at the most for the corresponding quantity of evaporated gold, can be excluded for several reasons. First, the “molecular” roughness of the amorphous film surface and its specific area should simply prevent the formation of a perfect bi- or trilayer. Second, the SIMS signals of the underlying molecules should be greatly attenuated and not enhanced if there were a perfect multilayer. This fast attenuation of the secondary species signal

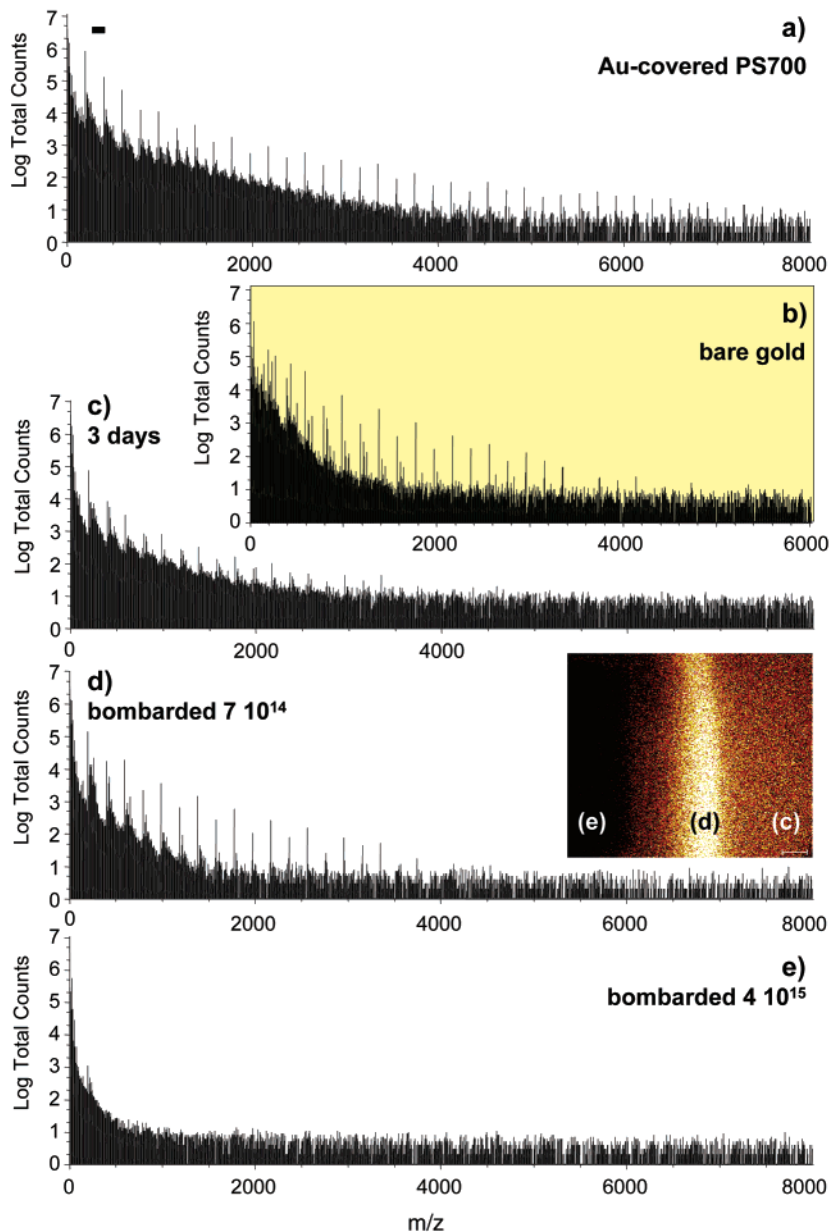


Figure 4. Negative secondary ion mass spectrum of (a) Au-metallized ( $6 \text{ nmol/cm}^2$ ) PS700 film, (b) sputter-cleaned gold surface ( $10^{16} \text{ ions/cm}^2$ ), (c) sample a after 3 days, (d) sample c bombarded with a  $\text{Ga}^+$  fluence of  $7 \times 10^{14} \text{ ions/cm}^2$  (see text for the description of the inset), sample d bombarded with a  $\text{Ga}^+$  fluence of  $3.3 \times 10^{15} \text{ ions/cm}^2$ .

with increasing depth of origin has been observed with metal<sup>31</sup> as well as organic surfaces.<sup>25,32</sup> Third, it is known from the literature that the growth of a metallic gold film on many organic surfaces, including PS,<sup>33</sup> tends to occur via a clustering process. A similar growth mechanism involving clusters/islands has also been elegantly demonstrated using transmission electron microscopy in the case of gold vapor deposited onto amorphous carbon,<sup>34</sup> as well as copper<sup>35,36</sup> and silver<sup>18</sup> evaporated onto poly-

(ethyleneterephthalate). Such a tridimensional growth mechanism is driven by the bond strength that is greater between the metal atoms themselves than between the metal atoms and the organic surface.

After 3 days, the negative mass spectrum of the same surface looks different (Figure 4c). The intensity of the gold clusters is reduced by an order of magnitude, and clusters containing more than 20 atoms cannot be detected anymore, indicating either a diffusion of the clusters toward the bulk or a migration of molecules over the gold clusters, both mechanisms appearing as two different views of a single phenomenon. An area of the same sample ( $400 \times 400 \mu\text{m}^2$ ) was submitted to a continuous  $\text{Ga}^+$  ion bombardment with a fluence of  $7 \times 10^{14} \text{ ions/cm}^2$ . The negative mass spectrum obtained afterward from the center of the sputtered

(31) Harrison, D. E.; Kelly, P. W.; Garrison, B. J.; Winograd, N. *Surf. Sci.* **1978**, *76*, 311.

(32) Beardmore, K.; Smith, R. *Nucl. Instrum. Methods B* **1995**, *102*, 223.

(33) Droulas, J. L.; Jugnet, Y.; Tran Minh Duc, In *Metallized Plastics 3*; Mittal, K. L., Ed.; Plenum Press: New York, 1992; p 123.

(34) Krakow, W. *Mater. Res. Soc. Symp. Proc.* **1992**, *237*, 447.

(35) Gollier, P.-A.; Bertrand, P. In *Polymer-Solid Interfaces: From Model to Real Systems*; Pireaux, J.-J., Delhalle J., Rudolf, P., Eds.; Presses Universitaires de Namur: Namur, 1998; p 173.

(36) Gollier, P.-A.; Bertrand, P. *J. Adhes. Sci. Technol.*, in press.

area is shown in Figure 4d. The intensity corresponding to gold clusters is partly restored in comparison with Figure 4c. This result suggests that the gold clusters/islands were sitting right underneath the top surface layer and were covered with a few molecular layers at the most. On the other hand, the spectrum of Figure 4d still does not exhibit gold clusters larger than Au<sub>20</sub>. It is therefore very similar to the mass spectrum of sputter-cleaned bare gold (Figure 4b). The explanation might be that gold clusters containing more than 20 atoms are present and easy to desorb as such after an hour (Figure 4a). For longer times, they might coalesce and form larger islands that are more difficult to dislocate (Figure 4c,d), much like a continuous gold surface (Figure 4b).

To check the vertical extent of the gold cluster/polymer interphase, a square of 260 × 260 μm<sup>2</sup> located in the center of the previously sputtered area was bombarded again with an ion fluence of 3.3 × 10<sup>15</sup> ions/cm<sup>2</sup>. The subsequent mass spectrum (Figure 4e) no longer exhibits any gold clusters, and shows only a weak signal of gold monocations. Figure 4e shows, then, that none of the gold clusters are able to diffuse deeper than a few monolayers, confirming that the driving force of the mechanism at play is the minimization of the surface free energy. The surface treatment of Figure 4c–e is summarized by the inset of Figure 4c, showing an image of the gold atomic ions emitted from the edge of the sputtered zone. The right part of the picture corresponds to the pristine sample after 3 days; the left part, to the central zone sputtered with a total fluence of 4 × 10<sup>15</sup> ions/cm<sup>2</sup>, and the middle part is the edge of the area that received primarily an intermediate fluence of 7 × 10<sup>14</sup> ions/cm<sup>2</sup>.

In summary, this analysis indicates that the organic surface metallized with 6 nmol/cm<sup>2</sup> of gold is covered with Au clusters forming islands. Complementary measurements with a PS700 sample covered with 20 nmol/cm<sup>2</sup> (not shown) confirm these observations. The structure obtained after evaporation is not stable, and the gold surfaces tend to be covered by organic molecules, reducing the surface free energy.

*Diffusion of Analyte Molecules over the Gold Clusters.* According to Hagenhoff,<sup>37</sup> the metal evaporation procedure is successful only when “the analyte is mobile and can diffuse on top of the evaporated metal layer”. It was shown in the previous section that diffusion processes indeed play a significant role in the freshly prepared Au-evaporated organic samples. Experimentally, it is difficult to study the diffusion of single molecules on the gold clusters, especially in the first hour following sample metallization, without in situ metallization equipment. Alternatively, we decided to monitor the diffusion of PS molecules from a monolayer cast on a gold substrate after sputter-cleaning a selected area of the substrate.

In practice, a dilute sample of PS700 was cast on a gold-metallized silicon wafer, and a 200-μm-wide area was prebombarded with an ion fluence close to 10<sup>16</sup> ions/cm<sup>2</sup>. Afterward, 10-min image acquisitions were conducted at regular time intervals on a 260 × 260 μm<sup>2</sup> area surrounding the prebombarded region. The results are summarized in Figure 5. The first column shows the images of Au-cationized PS tetramers, the lightest oligomers of PS700 in Figure 2, 10 min after prebombardment (Figure 5a)

and 1 h after prebombardment (Figure 5b). Figure 5a confirms that intact PS molecules have been removed from the central region of the analyzed area by the sputter-cleaning procedure. Nevertheless, after 10 min, the intensity arising from the border of the prebombarded area is slightly higher than that from the surrounding pristine sample. After an hour, this effect is reinforced, the intensity per pixel being several times larger at the frontier between the prebombarded area and the intact sample surface. The average intensity per pixel over two lines drawn across the images (numbered 1 and 2) is reported in two viewgraphs (second column, Figure 5c,d). On both edges cut by the linescans, the intensity corresponding to Au-cationized, intact PS tetramers is 3 times higher after 1 h (full line) than it was 10 min after sputter-cleaning (circles) and 5 times larger than it is in the undisturbed zone. In addition, it is clear from linescan 1 (Figure 5c) that the PS tetramer “front” is moving toward the sputter-cleaned area at a pace of several micrometers per hour. These results demonstrate unambiguously that small PS oligomers diffuse on the gold surface at a characteristic time that is comparable to the duration of the experiment. From this observation, it can be inferred that submicrometer gold clusters should be partly covered by short PS chains a few minutes after metallization already.

The same experiment was performed using PS2180. In this case, however, the results were inconclusive after an hour, that is, the maximum time spent between the Au-evaporation procedure and the SIMS analyses in our studies, suggesting that these larger molecules diffuse at least 10 times slower than PS700 on the sputter-cleaned gold surface. The much slower diffusion rate of PS2180 also explains why the molecular signals of PS700 and PS2180 behave differently as a function of the deposited metal quantity (Figure 3). Indeed, when they are metallized with 60 nmol/cm<sup>2</sup> of gold, the two samples do not recover in the same manner with time.

Another comment must be made concerning the experiment described in Figure 5. Even though short PS tetramers seem to diffuse quickly, the mass spectra show that the intensity ratio of consecutive oligomers in the distribution is as large as 10 in the diffusion front, as shown by the inset of Figure 5b. In other words, after an hour, the shape of the oligomer distribution in the diffusion front is completely altered, the tetramer peak being at least 1 order of magnitude more intense than the subsequent peaks. In comparison, the mass spectra showing the distributions of PS700 and PS2180 in Figure 2 (less than 1 h after metallization), which are quite similar to those obtained from a submonolayer on gold, and the fact that these distributions do not change significantly over a few hours suggest a state of quasi-equilibrium and not a kinetically driven situation, such as that reported in Figure 5 for the prebombarded PS monolayer on gold after 1 h. Therefore, in our opinion, the diffusion of PS molecules over the gold clusters is not the only reason for the mass spectra of intact molecules reported in Figure 2.

In summary, the diffusion of small PS oligomers over bare gold surfaces is a fact. Nevertheless, it does not seem to play the dominant role in the interpretation of the cationized oligomer distribution for PS2180 (Figure 2). For molecules under ~3 kDa, it is realistic to consider that the vicinity of organic molecules and gold atoms or clusters on the sample surface is a sufficient

(37) Hagenhoff, B. In *ToF-SIMS: Surface Analysis by Mass Spectrometry*, Vickerman, J. C., Briggs, D., Eds.; SurfaceSpectra/IMPublications: Manchester, 2001; p 285.

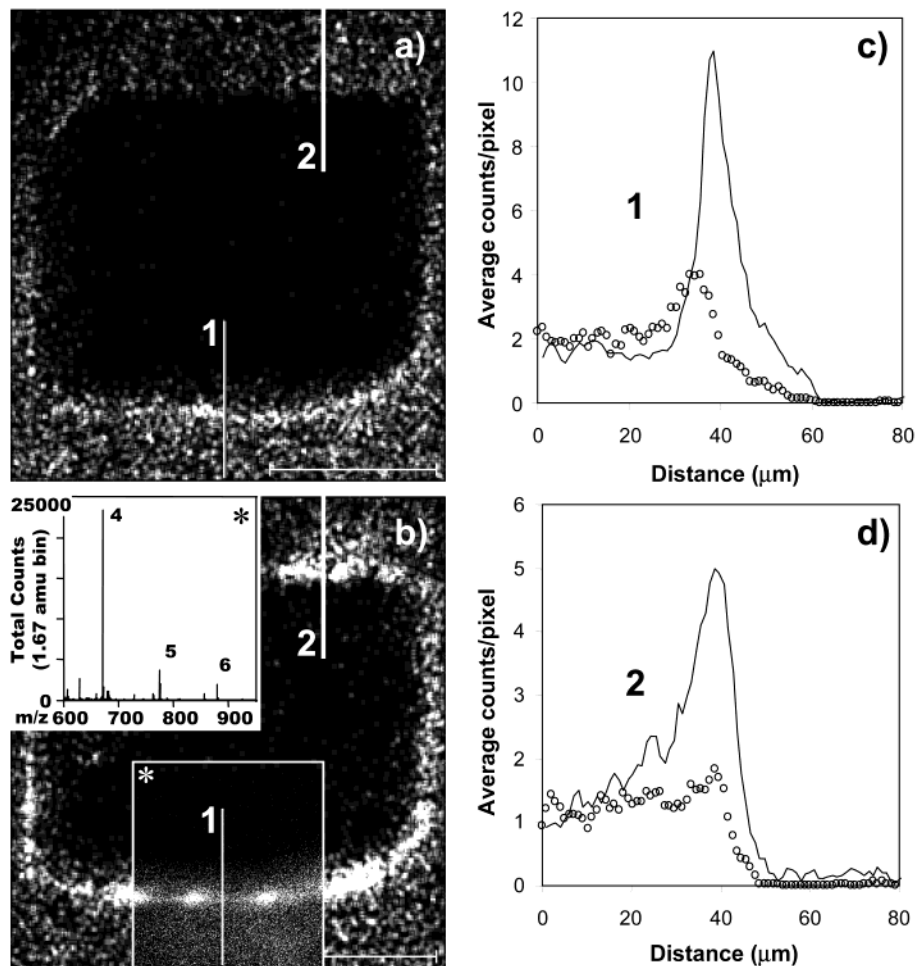


Figure 5. (a,b) Chemical mapping of PS tetramer molecules sputtered from a prebombarded ( $10^{16}$  ions/cm<sup>2</sup>) PS700 layer. Images of a  $260 \times 260 \mu\text{m}^2$  area surrounding the prebombarded region after (a) 600 s and (b) 3600 s (the top-left inset is the partial mass spectrum of the region marked by a star). (c)–(d) Intensity profiles measured along linescans 1 and 2 in frames a and b: circles, after 600 s; full lines, after 3600 s.

prerequisite for metal cationization. Even though the desorption of kilodalton molecules might be *facilitated* by the presence of an underlying metal surface, we believe that the intervention of a metal substrate is not an absolute *requirement*. This conclusion is strongly supported by recent MD simulation results in which kilodalton molecules<sup>38</sup> or polymeric chain segments<sup>39</sup> are sputtered from purely organic samples. In this framework, the simultaneous ejection of molecules and neighboring gold atoms in the same bombardment event might provide the necessary condition for cationization. Such a mechanism is supported by the experimental observation that oligomeric molecules can also be cationized by added alkali metals, such as Ni, K, or Na, irrespective of the organic layer thickness.<sup>37</sup> The case of larger molecules (beyond 3 kDa) is explored in the next subsection.

*Chain Entanglement: the Use of a Low-MW Matrix.* In the previous sections, we established that PS molecules heavier than  $\sim 3$  kDa could not be desorbed from the surface when prepared as a thick layer. Although diffusion effects involving the organic molecules and the gold clusters have been confirmed in the last two subsections, alone they do not explain the observed mass limit (3 kDa). Indeed, we showed that the strong reduction of

diffusion effects for molecules between 1 and 3 kDa does not prevent their ejection as cationized species. If the mass limit is not related to the absence of large molecule diffusion, it could be due to chain entanglement in the layer or the low efficiency of the sputtering process itself. To determine the influence of chain entanglement, we prepared a toluene solution containing 0.1 mg/mL of P4MS and 1 mg/mL of TPN as a matrix. The presence of the matrix is expected to help disentangle and isolate the polymer chains.

The positive mass spectrum of the metallized TPN/P4MS sample is shown in Figure 6. The first frame shows the fingerprint region of the spectrum, where  $\text{C}_8\text{H}_9^+$ , the most intense peak of P4MS, dominates. The middle frame of Figure 6 shows the intrinsically ionized TPN molecule, its Au-cationized homologue, and a series of aromatic fragments originating from this molecule. The bottom frame corresponds to the cationized P4MS oligomer region. Although the quantity of P4MS present on the sample surface is at least 1 order of magnitude lower with respect to the pure P4MS sample presented in Figure 2, the Au-cationized P4MS oligomers are clearly visible when the polymer sample is embedded in the TPN matrix. This result unambiguously demonstrates that the absence of Au-cationized P4MS molecules observed with the pure layer of P4MS is due to chain entanglement, not the

(38) Delcorte, A.; Garrison, B. J. *J. Phys. Chem. B*, submitted.

(39) Delcorte, A.; Bertrand, P.; Garrison, B. J. *J. Phys. Chem. B* **2001**, *105*, 9474.

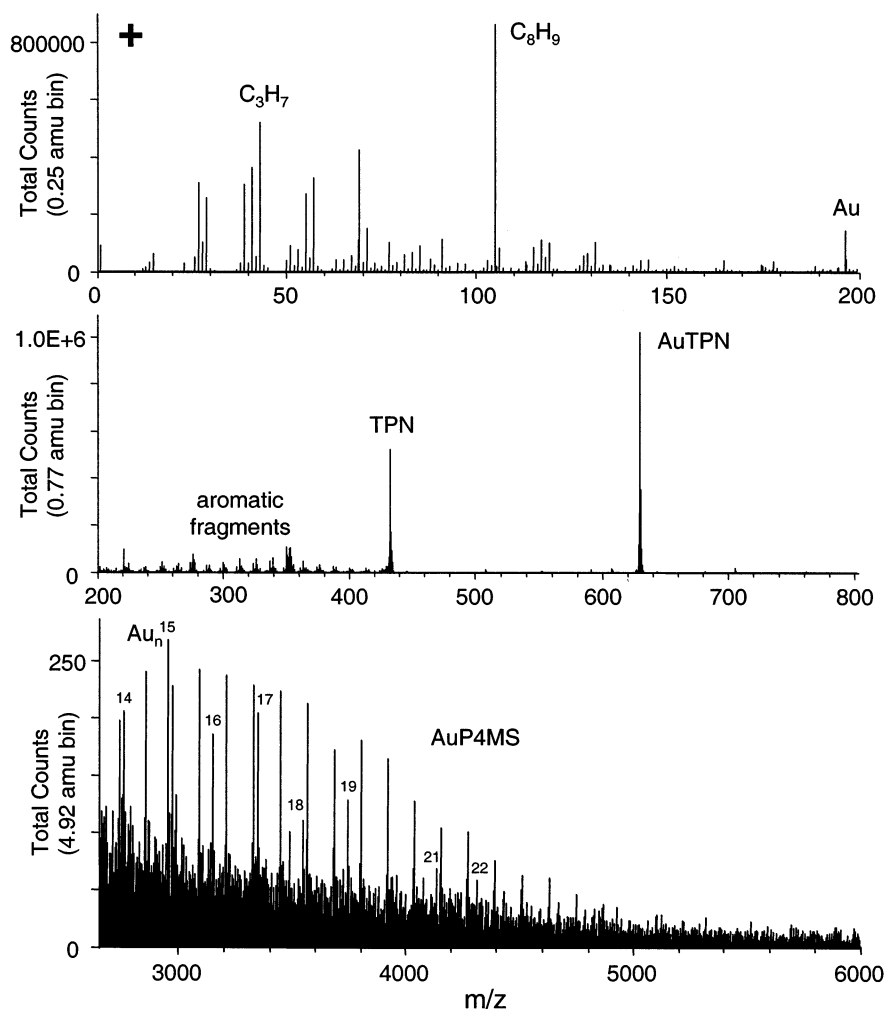


Figure 6. Positive secondary ion mass spectrum of a Au-metallized mixture of P4MS (0.1 mg/mL)/TPN (1 mg/mL).

slowing down of macromolecule diffusion on the surface or a strict theoretical limit regarding organic sample sputtering.

A significant issue for such a system concerns the possible segregation of one of the constituents at the surface of the blend. It is very difficult to draw any sensible conclusion about this question, because the two possible indicators of surface segregation in Figure 6 could be influenced by other effects. First, the fact that the molecular ion intensity ratio  $[I(\text{AuTPN})/\Sigma I(\text{AuP4MS}) \sim 5 \times 10^2]$  is significantly larger than the expected molar concentration ratio ( $\sim 10^2$ ) can probably be explained by the increased difficulty of sputtering larger molecules and the decrease in the detection efficiency with increasing mass. Indeed, a similar effect is observed with submonolayers on gold (Figure 2) where the possibility of segregation effects does not apply. Second, the shift of the P4MS distribution toward low masses in Figure 6 (with respect to Figure 2) could be simply due to the change from a metal substrate to a purely organic environment. Indeed, it has been unambiguously shown in a recent paper that, even for submonolayers of PS oligomers on metal surfaces, the shape of the MW distribution observed in SIMS is significantly dependent on the choice of the metal substrate.<sup>21</sup> Obviously, in that case, segregation effects are absent. The interpretation of this observation is that there is a mass dependence of the desorption and

ionization efficiencies, and this mass dependence varies with the nature of the substrate/environment.

**High-Molecular-Weight Polymers.** In the preceding sections, we focused our attention on the sputtering of limited size molecules and oligomers, typically with a molecular weight below 10 kDa. From the viewpoint of mass spectrometry analysis, they constitute an important application field, involving chemical, biological, and pharmaceutical compounds as well as low-molecular-weight polymers and polymer additives (see next section). Another large domain of applications, more specific to the SIMS technique, concerns high-molecular-weight polymers in the form of "real world" samples, such as films, containers, or molded parts. In the context of this study, we also wanted to assess the capability of the sample metallization procedure for the analysis of this type of sample. As shown in Table 1, three bulk samples made of high-molecular-weight polymers have been chosen for this purpose: a polyethylene (PE) bottle, a biaxially stretched polypropylene (PP) film, and a polystyrene (PSHM) Petri dish. The discussion will concentrate on the case study of the PE and PP samples, and a short comment will be made concerning the PSHM sample.

The positive secondary ion mass spectra of PE and PP are presented in Figure 7, each of them via three frames corresponding to analytically important mass ranges: the fingerprint region

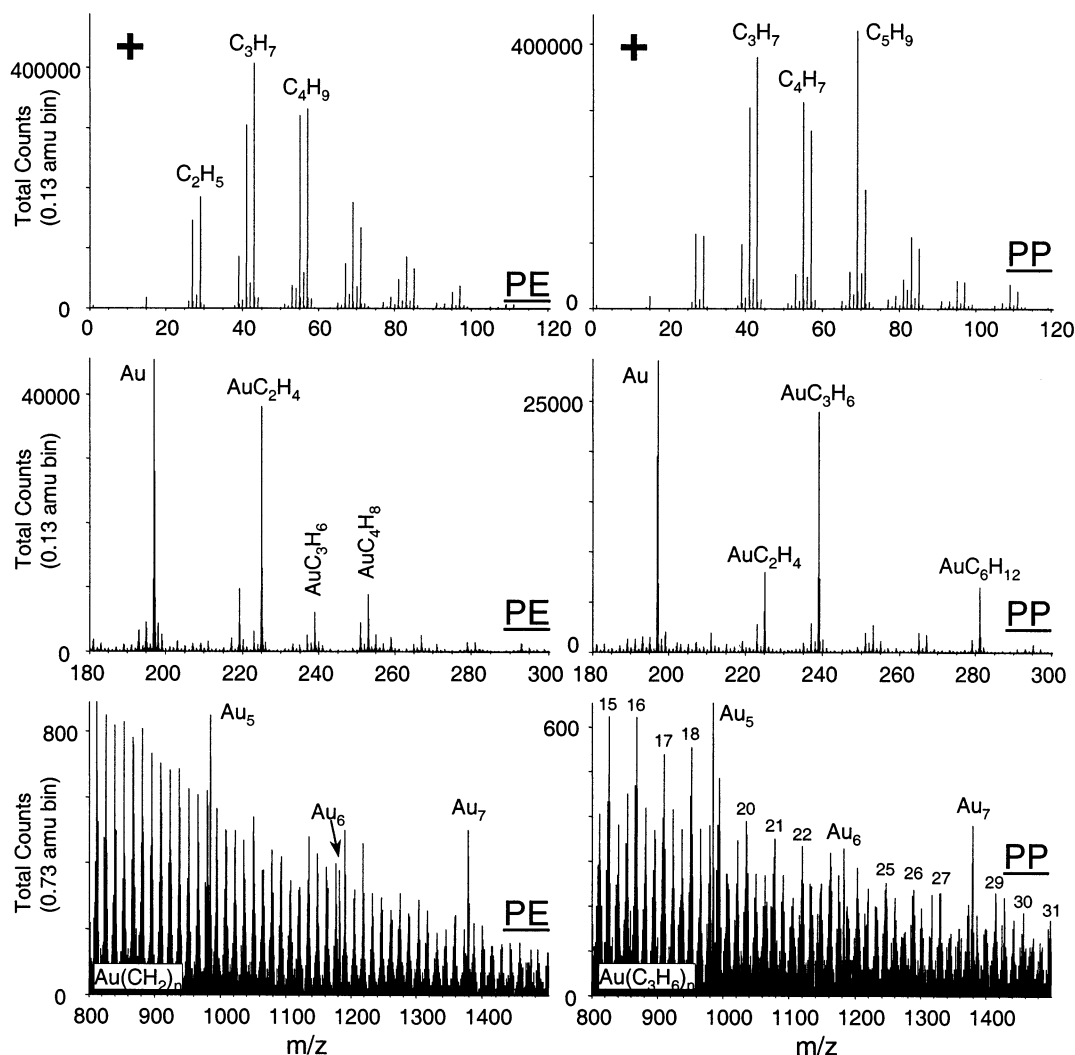


Figure 7. Positive secondary ion mass spectra of Au-metallized (20 nmol/cm<sup>2</sup>) bulk polyolefins. First column, polyethylene (PE) bottle; second column, polypropylene (PP) film.

( $0 < m/z < 120$ ); the gold monocation/Au-cationized monomer region ( $180 < m/z < 300$ ) and the Au cluster/Au-cationized chain segment region ( $800 < m/z < 1500$ ).

The fingerprint region of both samples is typical of saturated hydrocarbon polymers, with the highest intensities for peaks corresponding to  $C_nH_{2n+1}^+$  and  $C_nH_{2n-1}^+$  ions. Two observations must be made at this point. First, as is the case for pristine samples, PP and PE can be easily distinguished using the most characteristic peak of PP,  $C_5H_9^+$ , built on two repeat units of the polymer and stabilized by resonance as an ion. Thus, Au evaporation does not affect the fine spectral features of polyolefins that are traditionally used for characterization.<sup>29,40–43</sup> Second, the analysis of such insulating PE and PP samples without the Au-evaporation preprocessing requires the use of charge compensation (electron floodgun), and the secondary ion intensities are very low, around a few thousands counts, for these analysis conditions. In our case, no electron floodgun or grid were used. Despite the

simplicity of the characterization procedure, the secondary ion intensities were higher than  $4 \times 10^5$  counts for the most characteristic peaks of the fingerprint region, that is, more than 1 order of magnitude higher than the average intensities obtained for untreated samples. The case of PSHM, not shown, is similar; i.e., the fingerprint peaks of polystyrene,  $C_6H_5^+$ ,  $C_7H_7^+$ ,  $C_8H_9^+$ ,  $C_9H_7^+$ , and  $C_{15}H_{13}^+$  dominate the spectrum, and the intensity of  $C_7H_7^+$  is close to  $2 \times 10^5$  counts with the equipment and analysis conditions used in this study. In this respect, the metallization procedure certainly provides a significant enhancement of the sensitivity for thick, insulating samples.

The second region of interest ( $180 < m/z < 300$ ) comprises Au monocations and Au-cationized fragments. In addition to the  $Au^+$  peak, the most intense peaks in this region are  $AuC_2H_4^+$ ,  $AuC_4H_8^+$ , and  $AuC_3H_6^+$  for PE and  $AuC_3H_6^+$ ,  $AuC_6H_{12}^+$ , and  $AuC_2H_4^+$  for PP. The inversion of the relative intensities of  $AuC_2H_4^+$  and  $AuC_3H_6^+$  between the two samples is very significant, since  $C_2H_4$  is the repeat unit of PE and  $C_3H_6$  is the repeat unit of PP. Similarly,  $AuC_4H_8^+$  in the PE mass spectrum and  $AuC_6H_{12}^+$  in the PP mass spectrum include two repeat units of the respective polymers. Therefore, the Au-cationized fragments directly mirror

(40) van Ooij, W. J.; Brinkhuis, R. H. G. *Surf. Interface Anal.* **1988**, 11, 430.

(41) Briggs, D. *Surf. Interface Anal.* **1990**, 15, 734.

(42) Lianos, L.; Quet, C.; Tran, M. D. *Surf. Interface Anal.* **1994**, 21, 14.

(43) Delcorte, A.; Weng, L.-T.; Bertrand, P. *Nucl. Instrum. Meth. Phys. Res., Sect. B* **1995**, 100, 213.

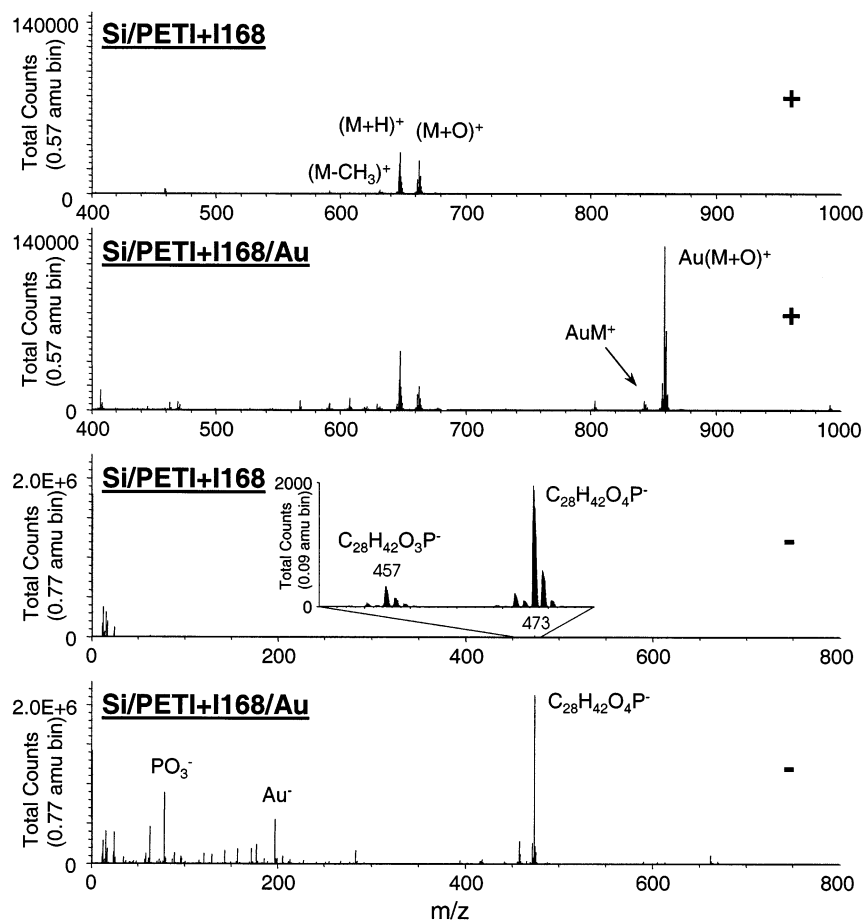


Figure 8. Effect of gold metallization (20 nmol/cm<sup>2</sup>) for a blend of poly(ethylene terephthalate/ethylene isophthalate) and Irgafos 168. Positive (top frames) and negative (bottom frames) mass spectra of the reference sample (Si/PETI + I168) and the Au-evaporated sample (Si/PETI + I168/Au).

the molecular structure of the polymer, and they can be used as a diagnostic to characterize the state of the surface.

The third important region ( $800 < m/z < 1500$ ) corresponds to kilodalton chain segments.<sup>39</sup> In addition to gold clusters, the mass spectrum of PE shows a series of peaks separated by 14 Da (CH<sub>2</sub>), corresponding to AuC<sub>n</sub>H<sub>2n</sub><sup>+</sup> clusters with  $44 < n < 94$ . These ions are long chain segments of polyethylene associated with a gold atom. The mass spectrum of PP exhibits the same series of peaks but with an additional feature. One out of three peaks in the series, corresponding to an ion including an integer number of PP repeat units, is more intense than the surrounding peaks. These ions, numbered in Figure 7, can be described by the formula Au(C<sub>3</sub>H<sub>6</sub>)<sub>n</sub><sup>+</sup> with  $15 < n < 31$ . Such large chain segments are not observed in the mass spectrum of untreated PE and PP samples, because they obviously need an extrinsic ionizing agent, for example, gold particles in our study. A glimpse into the microscopic mechanisms by which they detach and depart from the polymer is provided by the molecular dynamics simulations of Beardmore and Smith.<sup>32</sup> From an analytical viewpoint, the Au-cationized hydrocarbon segments, characteristic of the fine structure of the analyzed polymer, prove to be valuable. For instance, they provide a more direct discrimination between PE and PP samples.

**Polymer Additives.** Two polymer additives (antioxidants) have been analyzed in the context of this study: Irganox 1010

(I1010) and Irgafos 168 (I168) (see Table 1). The results are illustrated with the case of I168. The characterized sample is spin-cast from a solution of chloroform containing poly(ethylene terephthalate/ethylene isophthalate) (PETI, 30 mg/mL) and I168 (0.3 mg/mL).<sup>44,45</sup> Before analysis, the sample was stored for 6 months in ambient conditions in the context of a study aimed at determining the evolution of the antioxidant properties as related to aging time. One important feature of I168 is that it tends to segregate toward the PETI surface during the first few weeks following sample preparation, forming an enriched top layer that efficiently protects the polymer against oxidation. Therefore, despite its low concentration in solution, I168 is expected to be present in the TOF-SIMS spectra of the aged spin-cast blend.<sup>44,45</sup>

The partial positive mass spectrum of the Si/PETI + I168 system, encompassing the molecular ion mass range of the antioxidant, is shown in Figure 8 (first frame). As expected, the protonated molecule is the most intense peak in this region. Another important peak is the oxidized molecule [M + O]<sup>+</sup>, which is due to the reaction of the antioxidant with oxygen-containing species during the storage of the sample. The fragmented

(44) Médard, N.; Poleunis, C.; Vanden Eynde, X.; Bertrand, P. Proceedings of the European Conference on Applications of Surface and Interface Analysis (ECASIA01); *Surf. Interface. Anal. (special issue)*, in press.

(45) Médard, N.; Benninghoven, A.; Rading, D.; Licciardello, A.; Auditore, A.; Tran, M. D.; Montigaud, H.; Vernerey, F.; Poleunis, C.; Bertrand, P. *Appl. Surf. Sci.*, in press.

molecule peak resulting from the loss of a CH<sub>3</sub> residue is also present in this mass range at a lesser intensity.

The second frame of Figure 8 shows the positive TOF-SIMS spectrum of a similar sample after evaporation of 20 nmol of gold (Si/PETI + I168/Au). The three peaks mentioned above, [M + H]<sup>+</sup>, [M + O]<sup>+</sup>, and [M - CH<sub>3</sub>]<sup>+</sup>, exhibit an almost unchanged intensity with respect to the untreated sample. In addition to these ions, there is a large peak at *m/z* = 859 corresponding to the Au-cationized oxidized molecule, Au[M + O]<sup>+</sup>. The intensity of this peak is more than 5 times that of the [M + O]<sup>+</sup> ion. Remarkably, the Au-cationized antioxidant peak (AuM<sup>+</sup>; *m/z* = 843) is very weak with respect to Au[M + O]<sup>+</sup>. Because the recombination of three particles, M, O, and Au, during ejection is a low probability event, it is reasonable to consider that Au[M + O]<sup>+</sup> ions result almost exclusively from the recombination of gold atoms with I168 molecules that are already oxidized on the surface. In addition, the comparatively low intensity of the AuM<sup>+</sup> peak could indicate that a predominant fraction of the antioxidant molecules present on the PETI surface are oxidized. This interpretation makes sense, since the sample has been purposely kept in storage for 6 months, a sufficient amount of time for the antioxidant to diffuse toward the surface and to react with environmental moieties. Such an explanation could not be deduced from the relative intensities of [M + H]<sup>+</sup> and [M + O]<sup>+</sup>, because these two ions are formed by very different ionization mechanisms, and their intensities are also expected to be more strongly influenced by fragmentation reactions. At this point though, detailed considerations about this system are still somewhat speculative and a study aimed at verifying specific hypotheses is outside the scope of this article.

The negative mass spectrum of the Au-cationized sample also exhibits unusual features (fourth frame) as compared to the reference sample (third frame). Indeed, the oxidized I168 fragment peak, C<sub>28</sub>H<sub>42</sub>O<sub>4</sub>P<sup>-</sup>, which has an intensity (peak area) of 10 000 counts on the reference sample, is enhanced by a factor 200 on the Au-evaporated sample, where it actually dominates the entire mass spectrum (2.4 × 10<sup>6</sup> counts). The PO<sub>3</sub><sup>-</sup> fragment peak intensity is also drastically enhanced by gold evaporation. The reason for this enhancement could be related to the change of the sample band structure induced by the gold clusters present at the surface. The weakly bound electrons of the metal might recombine with the departing fragments at a relatively low energy cost.

A Au-metallized film of I1010 deposited on silicon has also been compared to an untreated film of the same antioxidant cast on iron. The details of the results are not shown here. Briefly, the Au-cationized molecule constitutes an intense peak in the high mass range of the positive mass spectrum, but there is no detectable parentlike ion peak in the mass spectrum of the untreated film. The fingerprint fragmentation peaks (below *m/z* = 200) are also 5 times more intense on average for the metallized film. The enhancement effect observed in the negative mass spectrum for I168 also occurs for I1010. For instance, the monomer fragment C<sub>17</sub>H<sub>25</sub>O<sub>3</sub><sup>-</sup> (*m/z* = 277) peak area is close to 1000 counts in the untreated sample mass spectrum, but it is >10<sup>5</sup> counts in the Au-metallized sample mass spectrum for the same analysis conditions.

In addition to pure hydrocarbon oligomers and polymers, the examples of I168 and I1010 show that metal cationization also provides valuable additional information (more diagnostic peaks, more intensity) in the case of chemically complex, heteroatom-containing molecules. It should be particularly powerful for real case studies, such as antioxidant diffusion and reaction at a polymer surface (PETI + I168), which would be impossible to conduct using submonolayers of organic material on metal substrates.

## CONCLUSION

In addition to submonolayer deposition of molecules on metals, this study shows that metal evaporation on top of organic surfaces constitutes an interesting alternative for sample cationization in SIMS. Beyond the specifics, the main advantage of this method is that it can be used whatever the thickness of the organic sample, opening the route toward cationization of "real world" samples (e.g., polymer film with additives) and chemical imaging applications. Surface mapping should not be influenced by the structure of the gold layer, granted that the metallic islands are nanometric and the lateral resolution of imaging SIMS instruments for organic samples is close to the micrometer.

For thick oligomer layers, the detection of cationized molecules can be performed up to a mass of ~3000 Da. The successful desorption of ~4000 Da poly(4-methyl styrene) oligomers embedded in a low-molecular-weight matrix shows that this apparent limit is partly due to chain entanglement in the pure oligomeric sample. Nevertheless, even in the case of oligomer samples in which entanglement prevents the detection of the cationized molecule, valuable information can be deduced from the presence and the yields of Au-cationized fragments. The study of polymer additives (antioxidants) shows that metal evaporation is also useful for the analysis of complex surfaces topped with heteroatom-containing molecules.

Another major interest of the method concerns high molecular weight, bulk polymers, for which the molecular ion is simply too large for intact desorption. In this case, the metal coverage, creating conducting paths, significantly enhances the fingerprint fragment intensities. It also gives rise to a new series of metal-cationized fragments that can be used for chemical diagnostic. Interestingly, the ionization of these fragments, induced by metal adducts, is less dependent on their chemical environment in the sample, and therefore, they should not be prone to matrix effects.

With respect to the metallization process, our study shows that the evaporated metal atoms form islands that tend to bury under (or to be covered by) the organic layer in a matter of days. Even though the results indicate that diffusion of small molecules (500 Da) on top of the gold surfaces certainly occurs much faster, the same could not be shown for larger molecules (2000 Da). Therefore, the need of molecule diffusion over the gold islands as a prerequisite to metal cationization, advocated by other authors is questionable. A scenario in which molecules or fragments associate with metal atoms from neighboring metallic clusters seems realistic, and it is theoretically supported, as well. To gain a better understanding of the metal molecule complexation in these systems, the kinetic energy distributions of sputtered species are also measured in our TOF-SIMS instrument, and a joint

experimental and theoretical study, including molecular dynamics simulations, is in preparation.

#### ACKNOWLEDGMENT

A.D. acknowledges the Belgian Fonds National pour la Recherche Scientifique, and N.M., the ADDIQUANTOF (contract GGRD-CT-1999-00158) research program of the European Community for financial support. The TOF-SIMS equipment was

acquired with the support of the Région Wallonne and FRFC-Loterie Nationale of Belgium.

Received for review February 26, 2002. Accepted June 27, 2002.

AC020125H